# Tropospheric NO2 columns: a comparison between model and retrieved data from GOME measurements

A. Lauer, M. Dameris, A. Richter, J. P. Burrows

▶ **To cite this version:**

A. Lauer, M. Dameris, A. Richter, J. P. Burrows. Tropospheric NO2 columns: a comparison between model and retrieved data from GOME measurements. Atmospheric Chemistry and Physics, 2002, 2 (1), pp.67-78. hal-00295186

**HAL Id: hal-00295186**
**https://hal.science/hal-00295186**

Submitted on 18 Jun 2008

**HAL** is a multi-disciplinary open access archive for the deposit and dissemination of scientific research documents, whether they are published or not. The documents may come from teaching and research institutions in France or abroad, or from public or private research centers.

L'archive ouverte pluridisciplinaire **HAL**, est destinée au dépôt et à la diffusion de documents scientifiques de niveau recherche, publiés ou non, émanant des établissements d'enseignement et de recherche français ou étrangers, des laboratoires publics ou privés.

Atmos. Chem. Phys., 2, 67–78, 2002
www.atmos-chem-phys.org/acp/2/67/

Atmospheric Chemistry and Physics

# Tropospheric $NO_2$ columns: a comparison between model and retrieved data from GOME measurements

**A. Lauer**[1], **M. Dameris**[1], **A. Richter**[2], **and J. P. Burrows**[2]

[1]DLR Institut für Physik der Atmosphäre, Oberpfaffenhofen, D-82234 Wessling, Germany
[2]Institut für Umweltphysik, Universität Bremen, D-28359 Bremen, Germany

Received: 31 October 2001 – Published in Atmos. Chem. Phys. Discuss.: 13 December 2001
Revised: 3 April 2002 – Accepted: 12 April 2002 – Published: 19 April 2002

**Abstract.** Tropospheric $NO_2$ plays a variety of significant roles in atmospheric chemistry. In the troposphere it is one of the most significant precursors of photochemical ozone ($O_3$) production and nitric acid ($HNO_3$). In this study tropospheric $NO_2$ columns were calculated by the fully coupled chemistry-climate model ECHAM4.L39(DLR)/CHEM. These have been compared with tropospheric $NO_2$ columns, retrieved using the tropospheric excess method from measurements by the Global Ozone Monitoring Experiment (GOME) of up-welling earthshine radiance and the extraterrestrial irradiance. GOME is part of the core payload of the second European Research Satellite (ERS-2). For this study the first five years of GOME measurements have been used. The period of five years of observational data is sufficiently long to facilitate for the first time a comparison based on climatological averages with global coverage, focussing on the geographical distribution of the tropospheric $NO_2$.

A new approach of analysing regional differences (i.e. on continental scales) by calculating individual averages for different environments provides more detailed information about specific $NO_x$ sources and of their seasonal variations. The results obtained enable the validity of the model $NO_2$ source distribution and the assumptions used to separate tropospheric and stratospheric parts of the $NO_2$ column amount from the satellite measurements to be investigated.

## 1 Introduction

Tropospheric $NO_2$ plays a key role in both stratospheric and tropospheric chemistry. In the troposphere the photolysis of $NO_2$ results in the formation of $O_3$ (e.g. Bradshaw et al., 2000). $NO_2$ can then be regenerated by catalytic cycles involving both organic peroxy radicals ($RO_2$), the hydroperoxyradical ($HO_2$), the hydroxyl radical (OH) and volatile organic compounds (VOC) and carbon monoxide (CO). In addition, $NO_2$ can react with $O_3$ to form the nitrate radical ($NO_3$), which is a strong oxidant and plays an important role, particularly in $NO_x$ polluted areas at night (Wayne, 1991). Thus $NO_2$ is one of the key species in determining the oxidising capacity of the troposphere. For more details on the role of $NO_2$ in atmospheric chemistry, the reader is referred to Finlayson-Pitts and Pitts (1999).

Although direct absorption of ultraviolet and visible radiation by tropospheric $NO_2$ is not thought to provide a large atmospheric forcing, local maxima of up to 0.1 to 0.15 $Wm^{-2}$ can be reached (Velders et al., 2001). As tropospheric $O_3$ is also a significant greenhouse gas, $NO_2$ also contributes indirectly to radiative forcing.

The emission of $NO_x$ ($NO_x = NO + NO_2$) into the troposphere is strongly influenced by human activities, $NO_x$ being produced in significant amounts by industrial combustion and biomass burning (Lee et al., 1997). Natural sources of $NO_x$ are lightning and emissions from soils in the troposphere. For further details on the contributions to the global $NO_x$ budget, see e.g. Brasseur et al. (1999). $NO_2$ is known to impact on human health and the environment both directly and through the production of $O_3$ (e.g. EPA, 2000). Overall it is necessary to monitor and understand the global impact of this pollutant on the physics and chemistry of the atmosphere.

The launch of GOME aboard the ERS-2 in April 1995 has enabled the global observation of the distribution of $NO_2$, which has significant amounts in both the stratosphere and the troposphere (Burrows et al., 1999). Further the development of the tropospheric excess method has enabled tropospheric $NO_2$ columns to be retrieved on scales up to global for the first time (Burrows et al., 1999), (Richter and Burrows, 2001). This retrieved data product provides a set of long-term observational data, which are well suited for evaluating the quality of the results of chemistry-climate models.

In this study, in contrast to recent studies by Leue et

*Correspondence to:* A. Lauer (Axel.Lauer@dlr.de)

© European Geophysical Society 2002

al. (2001) and Velders et al. (2001), climatological averages of the tropospheric $NO_2$ columns retrieved from GOME have been used. These have been compared with those obtained from the interactively coupled chemistry-climate model ECHAM4.L39(DLR)/CHEM on global and regional scales. Monthly average values of the $NO_2$ tropospheric columns retrieved using the TEM algorithm ("Tropospheric Excess Method") from five years of GOME observations (January 1996 to August 2000) and 20 years of model output provide the data base.

This comparison of modelled and measured tropospheric $NO_2$ column amounts is the first step in evaluating the ability of ECHAM4.L39(DLR)/CHEM to simulate the tropospheric $NO_x$ chemistry and to unveil still present deficiencies in chemistry and emission datasets. This first step is necessary to prepare future studies on the global impact of traffic (road and aircraft) induced $NO_x$ emissions on climate and air chemistry as well as their contribution to the global $NO_x$ budget in comparison to other man-made (industry and biomass burning) and natural (soils and lightning) $NO_x$ emissions. Once the chemistry-climate model ECHAM4.L39(DLR)/CHEM has been adjusted and evaluated to reproduce present and past global $NO_x$ measurements, prognostic simulations of future scenarios will be undertaken.

To achieve optimum comparability of the two different data sources, the satellite data have been fitted to the lower resolution of the model grid. The tropospheric $NO_2$ columns from the model data have been calculated in two ways:

1. Integration from the surface up to the (thermal) model tropopause ("Thermal Tropopause"-method).

2. Separation of tropospheric and stratospheric $NO_2$ amount using the method applied to the satellite data ("Tropospheric Excess or Reference Sector Method").

## 2 Data

### 2.1 Tropospheric $NO_2$ columns retrieved from GOME observations

GOME is a spectrometer on board ERS-2, which was launched on 20 April 1995 and flies in a sun-synchronous, polar orbit at an average height of 785 km above the Earth's surface (Burrows et al., 1999, and references therein). The GOME instrument observes in nadir viewing geometry the light (UV/visible) scattered back from the atmosphere and reflected at the ground. Once per day, it also observes the extraterrestrial solar irradiance. The instrument is designed to observe simultaneously the spectral range between 232 and 793 nm. The atmosphere is scanned with a spatial resolution of 320 km × 40 km (across track × along track) (forward scan) and 960 km × 40 km (back scan). Each individual orbit of ERS-2 takes about 100 min. Although the repeating cycle of an orbit is 35 days, nearly global coverage (except for a small gap around the poles) is achieved within three days applying the maximum scan width of 960 km (ESA, 1995). As a result of the sun-synchronous orbit, the measurements in low and middle latitudes are always taken at the same local time (LT) (the northern mid-latitudes are crossed at about 10:45 LT).

The trace gas retrieval of $NO_2$ is achieved using the DOAS technique (Differential Optical Absorption Spectroscopy). This technique utilizes the atmospheric absorption, defined as the natural logarithm of the ratio of the extraterrestrial irradiance and the earthshine radiance, for a selected spectral window. This is compared with reference absorption spectra of gases absorbing in the spectral window and a polynomial of low order. The polynomial describes the scattering and broad absorption in the window. The slant column of a gas is derived from the differential absorption of the gas in question and in first approximation is the integrated concentration along the light paths through the atmosphere. For this study, the spectral window from 425 to 450 nm has been used, the spectra of $NO_2$, $O_3$, $O_4$ and $H_2O$ and a reference Ring spectrum being fitted (Richter and Burrows, 2001).

The resultant slant columns of $NO_2$ can be converted to vertical columns by the application of an air mass factor, AMF. The AMF describes the effective length of the light path through the atmosphere and is derived from radiative transfer calculations. The value of the AMF depends on the viewing geometry and the solar zenith angle, but also on surface albedo, vertical gas profile, clouds and atmospheric aerosol. In this study, a constant vertical profile with all $NO_2$ in a 1.5 km boundary layer has been assumed. Stratospheric $NO_2$ is not included in the airmass factor calculation as the tropospheric slant columns have already been corrected for the stratospheric contribution, and the influence of stratospheric $NO_2$ on the radiative transfer can be neglected. (Richter and Burrows, 2001; Velders et al., 2001). A brief summary of the assumptions for derivation of the tropospheric $NO_2$ column amounts from the GOME measurements is given by Table 1.

The uncertainties introduced by the most relevant assumptions are discussed in Sect. 4.2. Details and a full error analysis can be found in Richter and Burrows (2001).

The Tropospheric Excess or Reference Sector Method for determining the tropospheric columns of $NO_2$ makes two assumptions:

a) the longitudinal distribution of stratospheric $NO_2$ is relatively homogeneous. This is reasonable at latitudes below 60° N through the year, because the bulk of the $NO_2$ in the stratosphere is at a relatively high altitude and as a result determined by photolysis and therefore mainly by day length which is a function of latitude only.

b) at remote locations over the Pacific, the tropospheric $NO_2$ column amounts are nearly constant and negligi-

**Table 1.** Summary of the assumptions for derivation of the tropospheric $NO_2$ column amounts from the GOME measurements (version 1.0 of the IUP/IFE-UB TEM $NO_2$ Dataset) (after Richter and Burrows, 2001). Negative values indicate error sources that tend to lead to an underestimation of the tropospheric $NO_2$

| Assumption | Purpose | Uncertainty |
|---|---|---|
| longitudinal homogeneity of the stratospheric $NO_2$ column amounts | separation of tropospheric and stratospheric amount (TEM) | $< 1 \times 10^{15}$ molec/cm$^2$ |
| constant and negligibly small tropospheric $NO_2$ column amounts in the reference sector above the Pacific at longitude 170° W to 180° W | separation of tropospheric and stratospheric amount (TEM) | $< 5 \times 10^{14}$ molec/cm$^2$ |
| constant vertical profile with all $NO_2$ in a 1.5 km boundary layer | tropospheric AMF calculation | ±50% |
| clear sky conditions | tropospheric AMF calculation | −30% |
| surface albedo of 0.05 | tropospheric AMF calculation | ±50% |
| $NO_2$ absorption cross-section for stratospheric temperatures (241 K) | $NO_2$ fit (DOAS) | −20% |

**Table 2.** Nitrogen Oxide emissions as used in the E39/C model simulation (Hein et al., 2001) and the range of uncertainty (Bradshaw et al., 2000)

| Source | Emissions [Tg(N)/yr] | Range [Tg(N)/yr] | Contribution [%] | Reference |
|---|---|---|---|---|
| Industry | 22.6 | 16–30 | 57.8 | Benkovitz et al. (1996) |
| Soils | 5.5 | 3–8 | 14.1 | Yienger and Levy (1995) |
| Lightning | 5.4 ± 0.1 (clim. annual mean) | 3.2–26[1] | 13.8 | Price and Rind (1992) |
| Biomassburning | 5.0 | 4–16 | 12.8 | Hao et al. (1990) |
| Aircraft | 0.6 | 0.5–0.6 | 1.5 | Schmitt and Brunner (1997) |
| Total | 39.1 | 26.7–80.6 | 100.0 | |

[1] free troposphere + near surface

bly small. This is shown by the results of aircraft measurements (Schultz et al., 1999) and by the GOME measurements themselves (Richter and Burrows, 2001).

Thus the TEM tropospheric columns of $NO_2$ are determined by subtracting the $NO_2$ column at a selected remote and clean location from that at other locations at the same latitude. In this study the reference clean sector is chosen to be around the international date line at longitude 180° W.

For this study, climatological monthly means of the tropospheric $NO_2$ column amounts (January 1996 to August 2000) have been used. The data were selected to be cloud free, i.e. only pixels having a cloud coverage below a threshold value 10% were used to derive the tropospheric $NO_2$ column amounts from the GOME measurements (see also Sect. 4.2). (Version 1.0 of the IUP/IFE-UB TEM $NO_2$ Dataset.)

## 2.2 ECHAM4.L39(DLR)/CHEM

ECHAM4.L39(DLR)/CHEM (hereafter referred to as E39/C) is a spectral atmospheric chemistry – general circulation model. The model consists of two parts, the atmosphere general circulation model ECHAM4.L39(DLR) (Land et al., 1999) and the chemistry module CHEM (Steil et al., 1998). ECHAM4.L39(DLR) and CHEM are fully coupled, facilitating the representation of feedback mechanisms between changes in concentrations of chemical species and the simulated dynamics. E39/C has a horizontal resolution of T30 (3.75° × 3.75°) and 39 layers in the vertical direction extending from the surface up to 10 hPa (30 km). The chemistry module CHEM includes 107 reactions and 37 trace gases in the troposphere and stratosphere. It is connected with the ECHAM4 radiation scheme via $H_2O$, $O_3$, $CH_4$, $N_2O$ and CFCs. The system thereby allows feedbacks between chemistry and the radiation scheme, which in turn, affects dynamics.

The current chemical scheme within CHEM does not include the $NO_x$ reservoir species PAN. In addition, CHEM neither includes VOC chemistry nor the heterogeneous reaction of $N_2O_5$ on the surface of wet aerosols in the troposphere forming $HNO_3$. This version of E39/C is specialized on stratospheric ozone chemistry. Nevertheless, this first look not only provides a detailed view into the current ability and deficiencies of E39/C to simulate tropospheric $NO_x$, but also enables the validation of the seasonal variation of currently used $NO_x$ emission data sets, as e.g. biomass burning. This step is essential to enable upcoming studies on

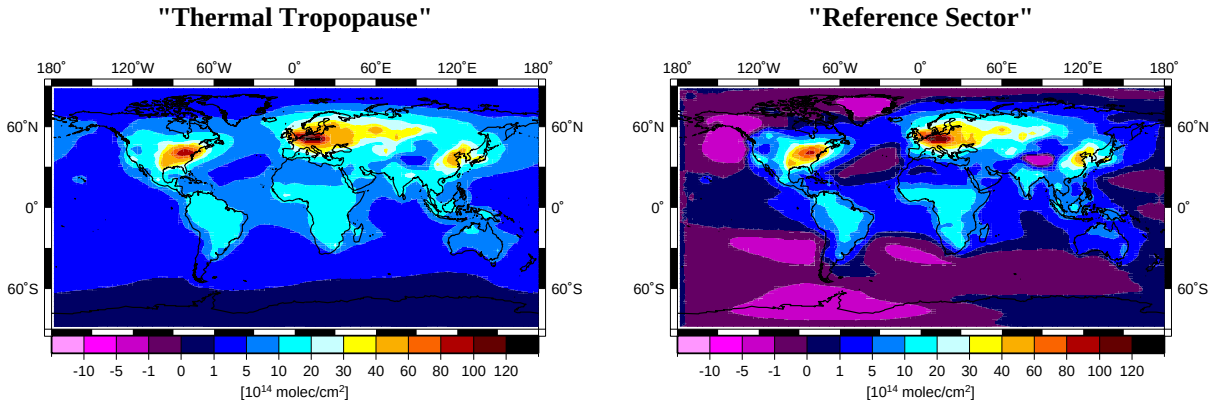


**Fig. 1.** E39/C, climatological annual means based on 20 years of the modelled tropospheric $NO_2$ column amounts, showing the results of the two different methods of calculation.

the present, past and future global impact of man-made $NO_x$ emissions (especially road-traffic and aircraft) in comparison to the natural (soils and lightning) $NO_x$ emissions not only on the climate (e.g. tropospheric $O_3$ production) but also on air chemistry (e.g. OH budget) and air quality.

Possible effects of the limitations on tropospheric $NO_x$ chemistry are discussed in Sect. 4.1.

For this study an existing dataset from the "1990" control experiment (Hein et al., 2001) has been used. The E39/C data used for this comparison represent the beginning of the 1990s. Therefore the model was run in quasi-equilibrium mode. Gas emissions, Sea Surface Temperature (SST), and boundary conditions were assumed similar to those measured or determined for the year 1990. A detailed model description and model applications can be found in Hein et al. (2001) and Schnadt et al. (2001).

Table 2 summarizes the Nitrogen Oxide emissions as considered for this model simulation. The total sum equals 39.1 Tg(N)/yr. The emissions from industry and ground based traffic, which are predominantly emitted by the eastern United States, Central Europe and Japan, have the major contribution of about 58% of the global budget. (This dataset is based on version 1A of the GEIA global inventories of the annual emissions of $NO_x$ from anthropogenic sources around the year 1985, Benkovitz et al., 1996). Especially in the tropics, biomass burning and lightning are the most important $NO_x$ sources. In addition emissions from soils and aircraft are explicitly taken into account.

## 3 Model data analyses and comparisons

In this study two methods have been used to calculate the tropospheric $NO_2$ columns from the model data. The first approach is to integrate the $NO_2$ concentration from the surface to the tropopause which is determined by employing the thermal WMO-criterion. This dataset is defined as the "Thermal Tropopause" dataset.

The second approach applies the TEM to the model data in a manner similar to that applied to the GOME observations. The averaged total column over a Pacific sector (170° W to 180° W) as estimate for the stratospheric amount (Richter and Burrows, 2001). The tropospheric column is calculated by subtracting this approximation of the stratospheric amount from the total columns.

The model results have been compared to each other. Although the "TEM" dataset yields smaller absolute values, the qualitative seasonal variation is not affected in any of the cases studied. Figure 1 shows the results of the two methods of calculation applied to the model output of E39/C. To calculate the climatological annual means, all 20 model years are used. As it can be seen easily, all major features of the global pattern are conserved. In both cases, the areas with high $NO_x$ emissions (namely United States, Central Europe and Southeast Asia/Japan) are clearly visible. Even the distribution of the patterns of regions with lower values of the tropospheric $NO_2$ column amounts (e.g. Africa, South America, Australia) are (in a qualitative sense) similar.

Comparison of the two different methods of calculation indicates that:

1. For the "Thermal Tropopause" dataset, the regions with high values of the tropospheric $NO_2$ column amounts have a somewhat larger extent and higher maximum values than the results of "TEM".

2. For the "TEM" dataset, negative values become possible in regions with low $NO_2$ column amounts, e.g. over the oceans.

3. In regions with very low tropospheric $NO_2$ column amounts (e.g. the oceans) "TEM" has a large inherent error resulting from subtraction of two similar quantities.

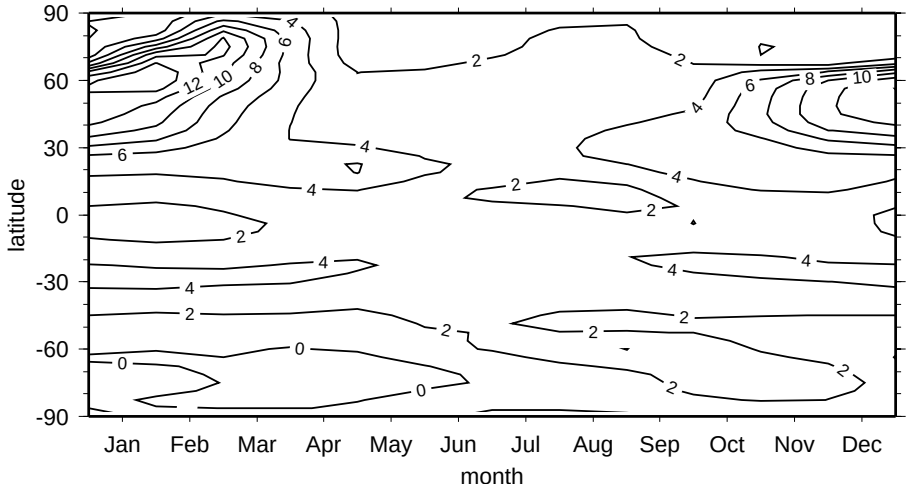


**Fig. 2.** Seasonal variation of the averaged climatological tropospheric $NO_2$ column amounts ($10^{14}$ molec/cm$^2$) for the reference sector over the Pacific Ocean (170° W to 180° W) as modelled by E39/C ("Thermal Tropopause"-method). In contrast, "TEM" assumes no tropospheric $NO_2$ being present in the reference sector.

4. The results over the continents are quite reasonable: the annual mean relative difference of both methods being below 30% for most of the examined regions.

The reason for the lower values obtained by TEM with model data is that significant concentrations of $NO_2$ are generated by the model at 170° W to 180° W. This appears to be outflow from the continents which is predominantly the case in the northern mid-latitudes in winter and results in a background of (1 to 7) $\times 10^{14}$ molec/cm$^2$ north of 60° S and $< 1 \times 10^{14}$ molec/cm$^2$ south of 60° S. In the remote maritime boundary layer assuming the height of the PBL to be 2 km this would correspond to 20 to 150 pptv. This may indicate that in the model the $NO_2$ is not being removed rapidly enough.

When looking at the model data one must keep in mind that the model domain does not extend above 10 hPa. Thus the stratospheric amounts calculated by the model do neither include $NO_2$ in the upper stratosphere nor in the mesosphere. This could reduce the total variability of the stratospheric columns by up to 1/3 and might also explain some of the variability over Antarctica, as seen in the TEM model data.

However, as mentioned before, the seasonal variation of the studied regions is not affected by "TEM", because (especially in the northern mid-latitudes in winter) the tropospheric $NO_2$ column amounts are several times higher than the overestimation of stratospheric $NO_2$ by the $NO_2$ above the reference sector. Figure 2 shows the averaged tropospheric $NO_2$ column amounts as modelled by E39/C above the reference sector over the Pacific Ocean.

### 3.1 Global comparison

For optimal comparison between the model results and the TEM dataset derived from GOME, in the following only model results obtained using TEM are compared to the GOME data (Fig. 3).

In January, both the satellite and the model data clearly show the large northern hemispheric $NO_x$ emission areas. These are caused by anthropogenic emissions from domestic heating, industry and road traffic: USA (particularly the eastern part), Europe and Southeast Asia/Japan. These areas can be easily identified by the high values of the tropospheric $NO_2$ column amounts.

A significant difference can be seen between the model- and satellite data in these regions: E39/C produces larger maxima and the regions of enhanced tropospheric $NO_2$ column amounts have a larger spatial extent than those observed in the satellite data.

On the other hand, the high $NO_2$ areas in central and southern Africa (caused by biomass burning and lightning produced $NO_x$) of both data sources are in good agreement: the location and the absolute column amounts being similar.

In January the GOME data show much higher variation of the $NO_2$ amounts over Antarctica than the model data (Fig. 3). Although the GOME data for Antarctica must be treated very carefully as not all assumptions made for the tropospheric $NO_2$ retrieval from the GOME measurements (see Table 1 and Sect. 4.2) are valid for this region, this might indicate widespread $NO_x$ emissions by sunlight from snow. The production of $NO_2$ in or just above snow is believed to result from the photolysis of $HNO_3$ carried to the Antarctic in the snow (e.g. Jones et al., 2001). This cycling mechanism is certainly not in the model yet, but the differential signal may be seen by GOME. The signal could be positive or negative

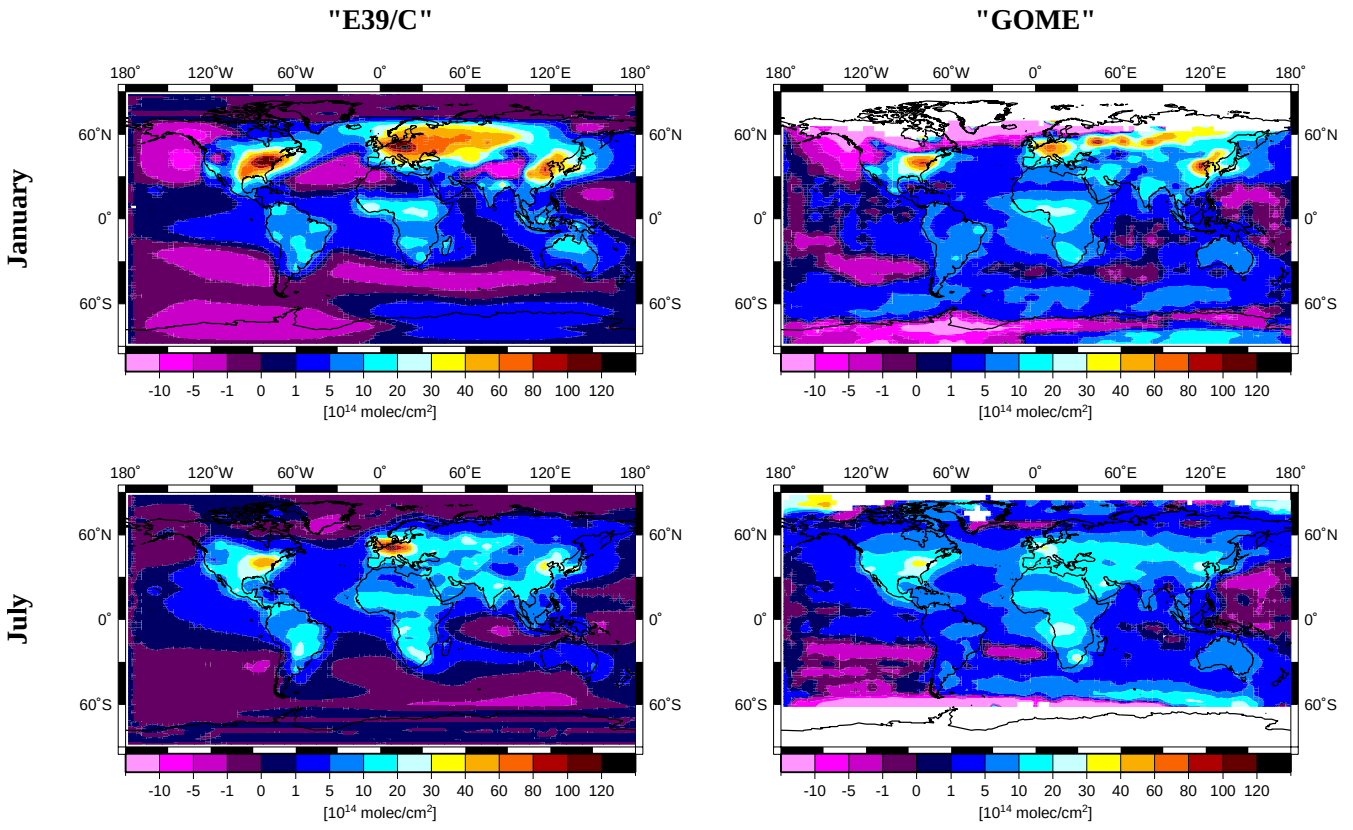


**Fig. 3.** Climatological monthly means of the tropospheric column amounts calculated by E39/C ('TEM') and derived from GOME measurements for January and July, respectively. Blank (white coloured) areas are data gaps.

in the TEM dataset, because it depends whether the region selected for the reference sector is producing some $NO_2$ by this mechanism or not. In addition, tropospheric $NO_x$ has a longer lifetime under these colder and probably low $O_3$ conditions. However, it has to be emphasized this is still very speculative at this stage.

In July, the tropospheric $NO_2$ column amounts reflect the reduction in the $NO_x$ emission in North America, Europe and Asia: both the magnitude of the $NO_2$ clouds and their areas being reduced in size in comparison to those of January. Again, these areas have a larger extent and higher maxima in the model data than shown by the GOME data.

These observations are in general consistent with the observation that relatively high $NO_2$ values are found at 180° E/W and above the oceans in the E39/C dataset. This seems to indicate that the model is not destroying $NO_x$ in the troposphere rapidly enough.

### 3.2 Analysis of the regional averages of $NO_2$ tropospheric columns

The tropospheric $NO_2$ columns exhibit a strong land-sea-contrast. To analyse regional differences and seasonal variations between the model and the TEM $NO_2$ GOME dataset, several regions of interest are chosen for further analysis (USA, Europe, Africa, Australia, South America, Southeast Asia/Japan) by selecting a suitable boundary. Each data point within this boundary that represents a $NO_2$ column above land is used to calculate a mean value for the domain. To differentiate between points over land and sea, the land-sea mask which is used by E39/C running at T30 resolution is utilized. This concept has been proven to give more reliable results when studying the seasonal variations than the standard method of calculating zonal means. This is explained primarily by the high spatial variability of the tropospheric $NO_2$ column amounts.

To investigate the sensitivity of the calculated mean tropospheric $NO_2$ column values to the selection of spatial boundaries, the average values for each domain were calculated for boundaries, which were diminished or enlarged by one or two pixels in each direction. This showed that the relative differences are typically negligibly small and in all cases, the qualitative characteristics of the seasonal variations were not affected (Lauer, 2001).

Figure 4 shows the results of the regional comparison. These can be summarized as follows:

– For the region 'Europe', E39/C and GOME show similar small seasonal variations, but the annual mean of the

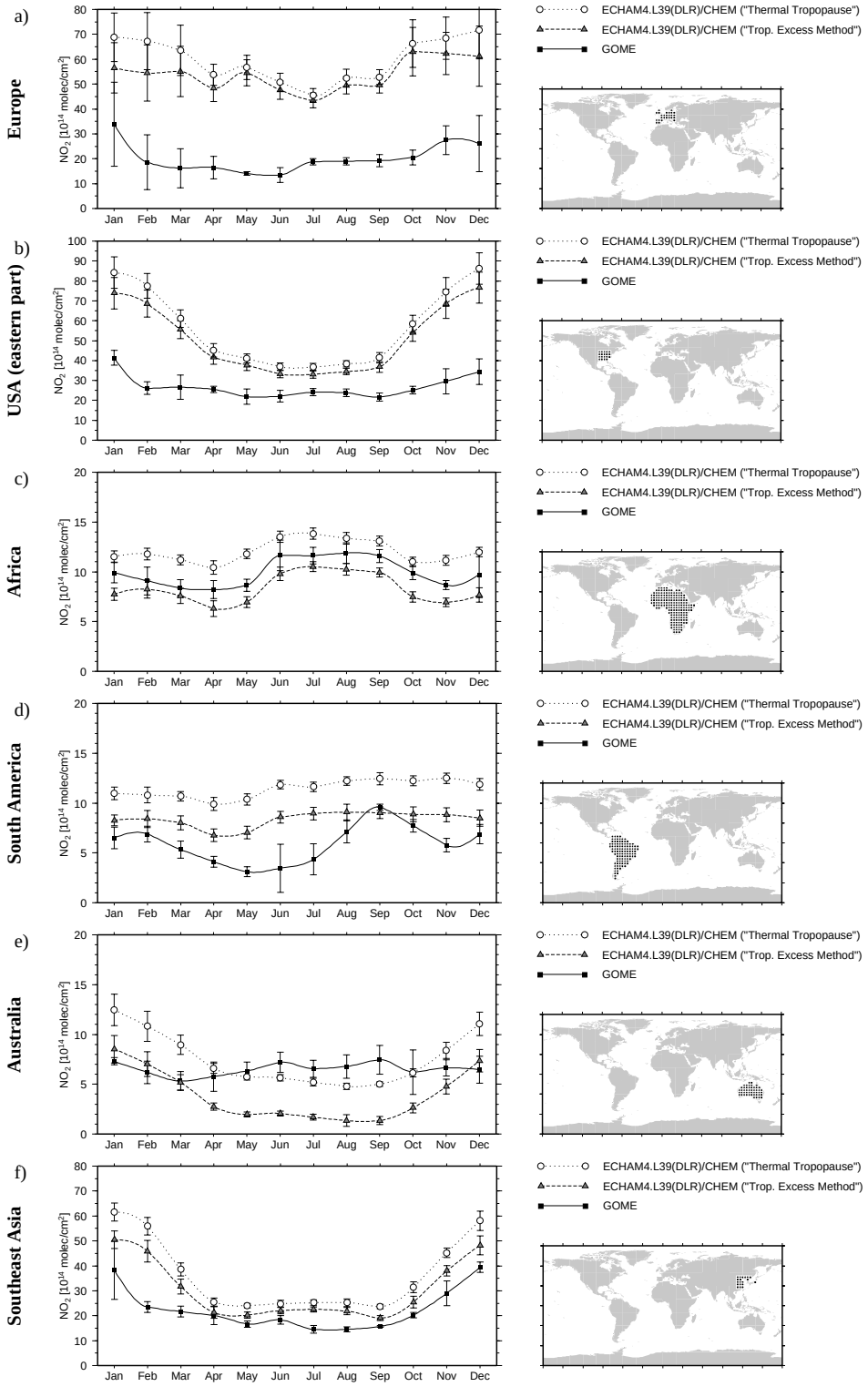


**Fig. 4.** (**a** – **f**): Seasonal variation of the tropospheric $NO_2$ column amounts for the climatological average values for selected spatial domains. The two sigma standard deviation of the individual monthly means to the climatological monthly means are drawn as errorbars for each data point. The small map to the right depicts the grid cells, that have been used to calculate the average values of the specified domain.

**Table 3.** Summary of the minimum, maximum and mean relative differences $r$ (given by Eq. 1) of the average values of the tropospheric $NO_2$ column amounts for the selected source regions. Positive (negative) values are corresponding to larger (smaller) column amounts by E39/C

| region | mean (%) | min. (%) | month | max. (%) | month |
|---|---|---|---|---|---|
| USA | 70.1 | 12.3 | (7) | 173.6 | (2) |
| USA (eastern part) | 90.5 | 37.6 | (7) | 162.7 | (2) |
| Europe | 164.7 | 66.6 | (1) | 287.4 | (5) |
| Africa | −16.6 | −9.1 | (2) | −24.3 | (10) |
| Central Africa | −3.7 | 0.1 | (8) | −18.6 | (11) |
| South Africa | −18.7 | −2.0 | (7) | −31.9 | (4) |
| South America | 41.7 | −5.7 | (9) | 148.3 | (6) |
| Australia | −40.4 | −2.4 | (3) | −81.8 | (9) |
| Southeast Asia/Japan | 34.8 | 6.1 | (4) | 95.4 | (2) |

results of E39/C ("TEM") is 2.65 times greater than that of GOME (Fig. 4a).

– In contrast to the GOME data, the model produces a relatively large and distinctive seasonal variation in the regions 'USA' (not shown) and '(eastern) USA' (Fig. 4b): maximum values occurring during the winter and minimum values during the summer. The results of E39/C show higher column amounts than the GOME data during the whole year, the annual mean is 1.7 times (USA) resp. 1.9 times ((eastern) USA) greater than that of GOME.

– The tropospheric $NO_2$ column amounts of E39/C and GOME for the region 'Africa' are both qualitatively and quantitatively similar. The annual mean of the GOME data is 1.2 times higher than that of E39/C ("TEM") (Fig. 4c).

– The tropospheric TEM $NO_2$ column amounts from GOME exhibit a distinctive seasonal variation for the region 'South America', having a minimum in May and a maximum in September. This is not reproduced by E39/C which shows only small seasonal variations. The annual mean of E39/C is 1.4 times greater than that of GOME (Fig. 4d).

– In 'Australia', the TEM $NO_2$ column data from GOME exhibit only a small seasonal variation, whereas E39/C shows a distinctive seasonal variation with minimum values occurring in winter and maximum values in summer. In contrast to the other regions, the model shows noticeably less $NO_2$ than the measurements during the winter months, when lightning activity is at its minimum. As lightning produced $NO_x$ is dominating the seasonal variation of the $NO_x$ emissions in the model (and therefore the seasonal variation of the tropospheric $NO_2$ column amounts), lightning produced $NO_x$ seems to be well represented by E39/C as there is good agreement between model and measurements during summer when the lightning activity is high. However, the other $NO_x$ sources seem to be too weak, particularly in winter. This could explain why the modelled $NO_2$ column amounts have lower values than the measured ones during the Australian winter. The annual mean of GOME is 1.7 times greater than that of E39/C (Fig. 4e).

– For the region 'Southeast Asia/Japan', the tropospheric $NO_2$ column amounts of E39/C and GOME are in good agreement. The only striking discrepancy is the month of February. Whereas the values of GOME go down rapidly from January to February, the decrease between January and February is shown by E39/C to a much lesser extent. The annual mean of E39/C is slightly higher than that of GOME, the relative difference being about 35% (Fig. 4f).

Table 3 summarizes the minimum, maximum and average relative difference of the TEM modelled and retrieved tropospheric $NO_2$ column amounts by E39/C and GOME, respectively. The relative difference $r$ is calculated by Eq. (1):

$$r = \frac{'\text{E39/C (TEM)}' - '\text{GOME}'}{'\text{GOME}'} \cdot 100\% \quad (1)$$

## 4 Discussion of results

There are several possible reasons for the observed differences between model and measurements. These can be divided into three basic error classes:

– model errors and deficiencies,

- errors from the GOME measurements and from the derivation of the tropospheric column amounts of the measured spectra,
- differences arising in the generation of the two data sources.

### 4.1 Model errors and deficiencies

How accurate and representative the model output is, depends on:

- the description of the atmospheric dynamics;
- the chemical scheme;
- the accuracy of the input data;
- the initialization data.

As $NO_2$ has a relatively short chemical short lifetime, the description of its chemical production and loss and the distribution and magnitude of sources are of significance.

The input sources are based on monthly means, which are assumed to remain constant during the whole period of simulation (20 years), except for lightning produced $NO_x$ which is related to the model's cloud parameterization scheme (Hein et al., 2001).

One of the main uncertainties in the calculated $NO_x$ volume mixing ratios, which are the basis for the calculation of the tropospheric $NO_2$ column amounts, are the uncertainties of the $NO_x$ emissions, both in the total amount and in the seasonal variation. Here, a simple phase shift of the used biomass burning dataset in the southern hemisphere (particularly South America and South Africa) by about one month could possibly improve the agreement of the modelled and observed seasonal variation of E39/C and GOME significantly (Lauer, 2001). In contrast, the seasonal variation of the biomass burning data set in (Northern) and Central Africa, which is dominating the seasonal variation of the total $NO_x$ emissions in this region seems to be quite good as the seasonal variation of the modelled and the observed tropospheric $NO_2$ column amounts are in good agreement.

In Australia, very low values of the $NO_2$ column amounts are modelled. As a direct result of the uncertainties of the emissions, the modelled tropospheric $NO_2$ has large uncertainties. Here, even slight changes of the emissions could give a different seasonal variation. Nevertheless, in summer when the lightning activity is high in Australia, there is good agreement between the two datasets both in the seasonal variation and in the absolute values for the column amounts. As the seasonal variation of the modelled $NO_2$ column amounts is clearly dominated by the lightning produced $NO_x$ emissions, the modelled lightning produced $NO_x$ seems to be appropriate. In addition to the general uncertainties of the $NO_x$ emissions, the datasets employed in the model have no daily variation, as e.g. caused by the rush hour in the morning and evening in Europe or the United States.

Even more important is the missing VOC chemistry and the missing $NO_x$ sink process 'heterogeneous reaction of $N_2O_5$ with $H_2O$ forming $HNO_3$' on the surface of tropospheric aerosols and at the Earth's surface.

The missing VOC chemistry prevents the formation of the $NO_x$ reservoir species PAN. A model study by Kuhn (1996) examined the impact of PAN on the $NO_x$ mixing ratios using the global 3-D Chemical Tracer Model, CTM, which has a horizontal resolution of $4° \times 5°$ and 9 vertical layers extending from the surface up to 10 hPa. Two model simulations, with and without taking into account PAN, were compared. The results showed, that PAN decreases (increases) the $NO_x$ mixing ratio in regions with high (low) $NO_x$ mixing ratio, e.g. above the continents (oceans). However, the results suggest the effect on the $NO_x$ mixing ratio is below 10% above continents (Kuhn, 1996), and therefore probably even less on the tropospheric $NO_2$ column amounts.

In contrast, the missing hydrolysis of $N_2O_5$ on tropospheric aerosols seems to be quite important, especially for the mid-latitudes. Dentener and Crutzen (1993) studied the impact of the reaction of $N_2O_5$ on tropospheric aerosols on the global distributions of $NO_x$, $O_3$ and OH using the global 3-D chemical tracer model Moguntia, which has a horizontal resolution of $10° \times 10°$ and 10 vertical layers at 100 hPa distance. They took into account the role of night time chemical reactions of $NO_3$ and $N_2O_5$ on aerosol surfaces and calculated the resulting loss in $NO_x$. Their results showed that this additional $NO_x$ sink reduces the NOX ($NOX = NO + NO_2 + NO_3 + N_2O_5 + HNO_4$) present in the boundary layer above the U.S. and Europe by about 50% in winter and about 20% in summer. The increased heterogeneous NOX removal in winter is due to long darkness and low temperatures during the winter months. For tropical regions, e.g. Africa, this process seems to be much less important and reduces the boundary layer NOX only about 10 to 30%. This can be explained by the increased importance of the daytime reaction of $NO_2$ with OH in tropical regions (Dentener and Crutzen, 1993).

In contrast, a study by Schultz et al. (2000) analysing aircraft measurements at 6–12 km altitude over the tropical South Pacific states that the $N_2O_5$ hydrolysis is less important (in the free troposphere over the tropical South Pacific) than previously assumed by other (modeling) studies. However, this is not contradictory to the conclusion of this study (based on the study of Dentener and Crutzen, 1993) on the effect of the $N_2O_5$ hydrolysis on the tropospheric $NO_2$ column amounts, as the major fraction of the tropospheric $NO_2$ column amounts is located in the boundary layer and lower troposphere and not in the free troposphere.

In Europe, North America and Asia, large quantities of $NO_x$ are released in winter into the planetary boundary layer. In the tropics convective activity pumps some of the $NO_x$ out of the planetary boundary layer and the lightning source releases $NO_x$ above the planetary boundary layer, where the lifetime of $NO_x$ is increased compared to the surface.

The current limitations within the model, describing the $NO_x$ emissions and the chemistry in the lower troposphere, appear strong candidates to explain the differences between model and retrieved datasets. Particularly the missing $N_2O_5$ hydrolysis should account for some of the overestimation of $NO_2$ by the model. The estimated size of the error (as stated by Dentener and Crutzen, 1993) is in good agreement with the observed differences.

### 4.2 GOME errors

Errors are introduced to the TEM $NO_2$ column dataset from GOME observations for two types of reason:

- Inherent uncertainties in the measurement itself and the retrieval of the trace gas concentration from the measured spectra.
- Remote sensing specific issues.

The errors from the measurement and the retrieval using DOAS are small in general and can usually be neglected compared to the other error sources.

In contrast, the errors due to remote-sensing specific problems are potentially more significant. To detect $NO_2$, GOME measures visible light (425 to 450 nm). The presence of clouds prevents the detection of $NO_2$ below the cloud, and enhances GOME's sensitivity for the detection of $NO_2$ above the cloud top. To minimize the impact of clouds, the retrieval of the TEM tropospheric $NO_2$ column amounts is restricted to atmospheric scenes having a cloud coverage below the threshold value 10%. This threshold value has been chosen to balance between meeting the needs of the 'clear sky' assumption in the AMF calculations and the number of available measurements. Because of the large dimension of the GOME pixels, the number of usable measurements would drop dramatically when using a lower threshold value.

Errors arising from undetected clouds (i.e. sub pixel scene) and cloud fractions below the threshold value may lead to an underestimation of tropospheric $NO_2$ by up to 40%, although in most cases, this error is well below this peak value (Richter and Burrows, 2001). The presence of large amounts of aerosols have a similar effect on the detection of $NO_2$ as clouds.

A study by Martin et al. (2001) showed the potential of further improvements on the retrieval of tropospheric $NO_2$ from the GOME measurements. A new approach of using a global 3-D model of tropospheric chemistry for the calculation of the vertical $NO_2$ profiles required to calculate the AMF instead of assuming a globally uniform vertical profile seems to improve the $NO_2$ retrieval. In addition, especially the new treatment of partly cloudy scenes should improve the retrieval of tropospheric $NO_2$. This new AMF formulation enables the quantitative retrieval for partly cloudy scenes (which is the case quite often because of the large dimensions of the individual GOME pixels) (Martin et al., 2001).

In addition, also the separation of the total column amounts into stratospheric and tropospheric part are a potential error source as additional assumptions have to be made. In order to see the effect on the tropospheric $NO_2$ column amounts of this method of calculation, the model data have been calculated using "TEM" as well.

### 4.3 Different assumptions in the creation of the two datasets

There are three major sources, which may result in differences when comparing the model- and satellite data and arise from differences in their:

- Temporal offset,
- exclusive use of clear sky conditions,
- sun synchronous orbit of ERS-2.

As mentioned above, all the input conditions used for the model runs are representative of the early 1990s, whereas the GOME measurements were taken between 1996 and 2000. Thus a temporal offset of several years exists between the periods represented by the model and measured by GOME. Changes of the anthropogenic $NO_x$ emissions resulting in different $NO_2$ concentrations might in part also explain the differences. However the uncertainties on the $NO_x$ emission datasets used as input for the model are in any case large (see Table 2).

For the GOME data, only clear sky (threshold value for the cloud coverage of 10%) pixels are accounted for. In contrast, the tropospheric $NO_2$ column amounts from the model output have been calculated without taking cloud effects or the cloud fraction within the model box explicitly into account.

The loss of $NO_x$ by the reaction of $N_2O_5$ on aerosol and on cloud, which is significant at night, has been discussed above. In addition as $NO_2$ is photolysed by the incoming solar ultraviolet radiation, the lack of cloud in the model and presence of some cloud in the measurement is likely to impact on the comparison. This effect is difficult to quantify, too, because of the large dimensions of the model boxes, only very few data points will remain after sorting out all values with a cloud fraction above 10%. Especially for the mid-latitudes, it might become impossible to calculate representative monthly means.

The probably most important fact making the comparison of the model- and satellite data difficult is the sun synchronous orbit of GOME's space platform, the ERS-2 satellite. Because of this, every measurement of GOME is performed at the same local time between 10:05 and 10:55 LT. This period coincides with the minimum of the daily lightning activity over the continents as shown by long term observations of the Optical Transient Detector, OTD (Kurz, 2001). The simulation E39/C only provides averaged $NO_2$ values. Thus the modelled 24 hours average of the lightning produced $NO_x$ will overestimate the $NO_x$ present in the late

morning. A 3-D chemical transport model study by Velders et al. (2001) indicates that the $NO_2$ tropospheric columns at 10:30 LT are about 80% of the values averaged over 24 hours for the region Europe and the U.S., about 50 to 70% for the regions South America and Africa.

## 5 Conclusions

Overall the differences in the $NO_2$ tropospheric columns as retrieved from GOME observations and calculated by the general circulation model E39/C are within a factor of 2 to 3. The likely overestimation of the $NO_x$ in the GCM is probably best explained by the lack of the heterogeneous loss of $NO_x$ through the reaction of $N_2O_5$ with $H_2O$ on aerosols and clouds in the lower troposphere. Thus, extending the chemistry module CHEM to properly handle the heterogeneous $N_2O_5$ chemistry should be the next step in improving E39/C to perform simulations of tropospheric $NO_x$.

In spite of the deficiencies and various error sources of both model and satellite data, this investigation shows clearly the potential for testing the current capability of general circulation models to simulate the behaviour of the troposphere using satellite observations.

The major features of this first look can be summarized as follows:

In the northern mid-latitudes (USA, Europe), emissions from industry and ground based traffic are the most important source for $NO_x$.

In the tropics, especially biomass burning and emissions from lightning are the dominant $NO_x$ sources. Here, the seasonal variation, as well as the quantitative column amounts are in better agreement than for the USA and Europe. This is consistent with the conclusion of Dentener and Crutzen (1993) stating much lesser influence of the still missing additional $NO_x$ sink in the tropics. The better agreement in these regions also indicates that the prescribed biomass burning and lightning produced $NO_x$ emissions are quite reasonable.

*Acknowledgements.* This work is a contribution to TROPOSAT (EUROTRAC-2). It has been funded in part by the University and State of Bremen, the Ludwig-Maximilians-University München, the German Aerospace Center (DLR) and the European Union through the TRADEOFF and POET projects. The provision of level 1 GOME data by ESA for this scientific study is acknowledged.

## References

Benkovitz, C. M., Scholtz, M. T. , Pacyana, J., Tarrason, L., Dignon, J, Voldner, E. C., Spiro, P. A., Logan, J. A., and Graedel, T. E.: Global gridded inventories of anthropogenic emissions of sulfur and nitrogen, J. Geophys. Res., 101(D), 29 239–29 253, 1996.

Bradshaw, J., Davis, D., Grodzinsky, G., Smyth, S., Newell, R., Sandholm, S., and Liu, S.: Observed distributions of nitrogen oxides in the remote free troposphere from the NASA Global Tropospheric Experiment programs, Rev. Geophys., 38, 61–116, 2000.

Brasseur, G. P., Orlando, J. J., and Tyndall, G. S.: Atmospheric Chemistry and Global Change, Oxford Univ Pr (Sd), ISBN 0195105214, 1999.

Burrows, J. P., Weber, M., Buchwitz, M., Rozanov, V., Ladstätter-Weißenmayer, A., Richter, A., DeBeek, R., Hoogen, R., Bramstedt, K., Eichmann, K. -U., Eisinger, M., and Perner, D.: The Global Ozone Monitoring Experiment (GOME): Mission Concept and First Scientific Results, J. Atmos. Sci., 56, 151–175, 1999.

Dentener, F. J. and Crutzen, P. J.: Reaction of $N_2O_5$ on Tropospheric Aerosols: Impact on the Global Distributions of $NO_x$, $O_3$ and OH, J. Geophys. Res., 98(D4), 7149–7163, 1993.

EPA (United States Environmental Protection Agency): Air Quality Index – A Guide to Air Quality and Your Health, Washington D. C., 20460, EPA-454/R-00-005, 2000.

ESA (European Space Agency): GOME Global Ozone Monitoring Experiment users manual, ESA SP-1182, ESA/ESTEC, Noordwijk, Netherlands, ISBN 92-9092-327-x, 1995.

Finlayson-Pitts, B. J. and Pitts, J. N., Jr.: Chemistry of the Upper and Lower Atmosphere, Academic Press, ISBN 012257060X, 1999.

Hao, W. M., Liu, M.-H., and Crutzen, P. J.: Estimates of annual and regional releases of $CO_2$ and other traces gases to the atmosphere from fires in the tropics, based on the FAO statistics for the period 1975–1980, in Fire in the Tropical Biota, Ecological Studies, Vol. 84, (Ed) Goldammer, J. G., 440–462, Springer-Verlag, New York, 1990.

Hein, R., Dameris, M., Schnadt, C., Land, C., Grewe, V., Köhler, I., Ponater, M., Sausen, R., Steil, B., Landgraf, J., and Brühl, C.: Results of an interactively coupled atmospheric chemistry-general circulation model: Comparison with observations, Ann. Geophysicae, 19, 435–457, 2001.

Jones, A. E., Weller, R., Anderson, P. S., Jacobi, H.-W., Wolff, E. W., and Schrems, O.: Measurements of $NO_x$ emissions from Antarctic snowpack, Geophys. Res. Lett., 28, 1499–1502, 2001.

Kuhn, M.: Untersuchungen zur troposphärischen Verteilung von Stickoxiden, Ozon, OH, Peroxiden, Aldehyden und PAN mit einem dreidimensionalen globalen Chemie- und Transportmodell, Ph.D. thesis, Mathematisch-Naturwissenschaftliche Fakultät der Universität zu Köln, Köln, 1996.

Kurz, C.: $NO_x$-Produktion durch Blitze und die Auswirkung auf die globale Chemie der Atmosphäre, diploma thesis, Meteorologisches Institut der Universität München, München, 2001.

Land, C., Ponater, M., Sausen, R., and Roeckner, E.: The ECHAM4.L39(DLR) atmosphere GCM – Technical description and model climatology, Report No. 1991-31, DLR Oberpfaffenhofen, Wessling, Germany, ISSN 1434-8454, 1999.

Lauer, A.: Untersuchungen der geographischen und jahreszeitlichen Variationen von troposphärischen $NO_2$ Säulen – Vergleich von Modell- und Satellitendaten, diploma thesis, Meteorologisches Institut der Universität München, München, 2001.

Lee, D. S., Köhler, I., Grobler, E., Rohrer, F., Sausen, R., Gallardo-Klenner, L., Olivier, J. G. J., Dentener, F. J., and Bouwman, A. F.: Estimations of global $NO_x$ emissions and their uncertainties, Atmos. Environ., 31, 1735–1749, 1997.

Leue, C., Wenig, M., Wagner, T., Klimm, O., Platt, U., and Jähne, B.: Quantitative analysis of $NO_x$ emissions from Global Ozone Monitoring Experiment satellite image sequences, J. Geophys. Res., 106, 5493–5505, 2001.

Martin, R. V., Chance, K., Jacob, D. J., Kurosu, T. P., Spurr, R. J. D., Bucsela, E., Gleason, J. F., Palmer, P. I., Bey, I., Fiore, A. M., Li, Q., and Yantosca, R. M.: An Improved Retrieval of Tropospheric Nitrogen Dioxide from GOME, submitted to J. Geophys. Res., 2001.

Price, C. and Rind, D.: A Simple Lightning Parameterization for Calculating Global Lightning Distributions, J. Geophys. Res., 97(D), 9919–9933, 1992.

Richter, A. and Burrows, J. P.: Tropospheric $NO_2$ from GOME measurements, Adv. Space Res., in press, 2001.

Schmitt, A. and Brunner, B.: Emissions from aviation and their development over time, in Pollutants from air traffic – results of atmospheric research 1992-1997, DLR-Mitt. 97-04, (Eds) Schumann, U., et al., 37–52, DLR Köln, 1997.

Schnadt, C., Dameris, M., Ponater, M., Hein, R., Grewe, V., and Steil, B.: Interaction of atmospheric chemistry and climate and its impact on stratospheric ozone, Clim. Dyn., in press, 2001.

Schultz, M. G., Jacob, D. J., Wang, Y., Logan, J. A., Atlas, E. L., Blake, D. R., Blake, N. J., Bradshaw J. D., Browell, E. V., Fenn, M. A., Flocke, F., Gregory, G. L., Heikes, B. G., Sachse, G. W., Sandholm, S. T., Shetter, R. E., Singh, H. B., and Talbot, R. W.: On the origin of tropospheric ozone and $NO_x$ over the tropical South Pacific, J. Geophys. Res., 104, 5 829–5 843, 1999.

Schultz, M. G., Jacob, D. J., Bradshaw, J. D., Sandholm, S. T., Dibb, E. J., Talbot, R. W., and Singh, H. B.: Chemical $NO_x$ budget in the upper troposphere over the tropical South Pacific, J. Geophys. Res., 105, 6 669–6 679, 2000.

Steil, B., Dameris, M., Brühl, C., Crutzen, P. J., Grewe, V., Ponater, M., and Sausen, R.: Development of a chemistry module for GCMs: first results of a multiannual integration, Ann. Geophysicae, 16, 205–228, 1998.

Velders, G. J. M., Granier, C., Portmann, R. W., Pfeilsticker, K., Wenig, M., Wagner, T., Platt, U., Richter, A., and Burrows, J. P.: Global tropospheric $NO_2$ column distributions: Comparing 3-D model calculations with GOME measurements, J. Geophys. Res., 106, 12 643–12 660, 2001.

Wayne, R. P. (Ed): The nitrate radical: physics, chemistry, and the atmosphere, Atmos. Environ., 25, 1–203, 1991.

Yienger, J. J. and Levy, H.: Empirical model of global soil-biogenic $NO_x$ emissions, J. Geophys. Res., 100(D), 11 447–11 464, 1995.